電気材料技術雑誌 第10巻第2号
J. Soc. Elect. Mat. Eng. Vol. 10, No. 2, 2001

InAs-based single-electron transistor fabrication using AFM oxidation

S. Sasa and M. Inoue

Department of Electrical Engineering, Osaka Institute of Technology,
5-16-1 Ohmiya, Asahi-ku, Osaka 535-8585, Japan

Abstract

We describe atomic force microscope (AFM) oxidation process which is particularly useful for nanofabrication of InAs/AlGaSb heterostructures. The fabrication process is based on anodization that occurs between the AFM tip and the InAs surface layer. We show that the oxidation turns the InAs into an insulator that can be used as a gate insulator for the fabrication of in-plane-gate FET structures. A single-electron transistor was fabricated in order to demonstrate the simple and useful nanofabrication capability of the AFM oxidation process. The device characteristics verify the successful operation as a single-electron transistor.

I. Introduction

Nanofabrication utilizing a scanning probe microscope (SPM) has become a useful tool for the exploration of new types of nanostructure devices such as single electron transistors (SETs). An SPM oxidation process on silicon surfaces was first demonstrated by Dagata *et al.*[1] and was then applied to GaAs by Snow *et al.*,[2] a compound semiconductor heterostructure,[3] and metal nanofabrication.[4] Since InAs has a small electron effective mass, a large quantum effect is expected to appear at a relatively large lateral confinement size of about 100 nm.[5]

We have investigated the applicability of an atomic force microscope (AFM) oxidation process on high-mobility InAs/AlGaSb heterostructures for the first time.[6] Various kinds of nanofabrication processes based on AFM oxidation are developed. For lateral periodic structure formation, GaSb oxidation and successive water immersion provides a simple and useful fabrication process. The magnetoresistance signal showed that successful modification of the two-dimensional electron gas (2DEG) potential with the lateral period corresponding to the modification period is achieved. For the fabrication of the InAs channel layer, GaSb/AlGaSb oxidation and developer solution etching is applied. InAs selective etching is then used with the fabricated GaSb/AlGaSb layer as the pattern transfer mask. An SET structure and the device characteristics are presented. We also describe AFM oxidation of InAs for the fabrication of an SET with a reduced fabrication size compared to AFM oxidation process based on Sb-based layer oxidation. Since the oxidation turns the InAs into an insulator, this provides a simple and advantageous nanofabrication technique for the development of InAs-based SETs.[7] The fabrication process enabled the formation of a reduced fabrication size smaller than 0.1 μm by eliminating pattern transfer processes indispensable for the fabrication of Sb-based layers in InAs/AlGaSb heterostructures. In addition, the fabrication process eliminates precise control on the oxidation depth and on the successive etching of the InAs layer. An SET structure and the device performance indicating the successful formation and usefulness of the AFM oxidation process are shown.

II. Experimental

1) Sample preparation

The InAs/AlGaSb heterostructure used in this experiment was grown by molecular beam epitaxy (MBE). The structure consists of a 0.75-μm-thick AlSb buffer layer, a 15-period GaSb (6 nm)/AlSb (6 nm) superlattice (SL) layer, a 200-nm-thick AlGaSb layer, a 16-nm-thick AlSb layer, a 15-nm-thick InAs channel layer, and AlGaSb (15 nm)/GaSb (10 nm) surface layers. The structure is grown on a semi-insulating (100) GaAs substrate. The growth temperature for both the AlSb buffer and the SL layers was 580°C. It was decreased down to 450°C prior to the initiation of the InAs growth. The AlGaSb/GaSb surface layers were grown to prevent the InAs channel layers from exposure to air before the AFM fabrication process.

2) AFM oxidation of InAs, GaSb, and AlGaSb

Oxidation characteristics for each constituent material in the heterostructure were studied. AFM oxidation was carried out by scanning a negatively-biased Au-coated conducting tip over the sample surfaces with applied biases up to 30 V. AFM was operated in air with a constant scan speed of 10 nm/s. AFM was operated in air with a constant scan

speed of 10 nm/s. The humidity was kept between 50 to 60% to facilitate the oxidation. We found that oxidation occurs for all the materials. Figure 1 compares the oxidation characteristics for InAs and GaSb measured by the height increase after AFM oxidation. The oxidation for InAs and GaSb was, as is shown, accompanied with a prominent volume increase while for AlGaSb noticeable volume increase was not observed. As can be seen in the Fig. 1, the threshold voltage for oxidation, V_{TOX} depends on the material. In contrast to conventional anodic oxidation, the unintentionally n-doped InAs showed the lowest V_{TOX} of less than 5 V and the unintentionally p-doped GaSb and AlGaSb showed higher V_{TOX} for AFM oxidation.

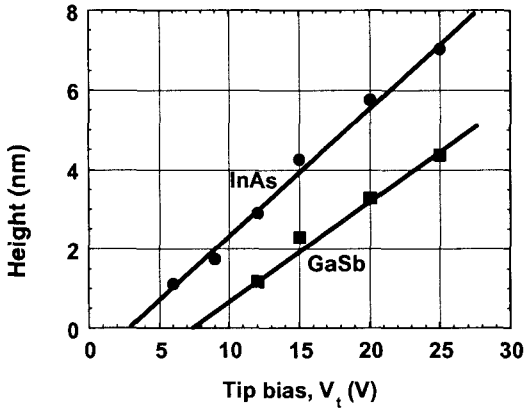

Fig. 1 Height increase after AFM oxidation for InAs and GaSb. The increase linearly varies as a function of tip bias.

3) Characterization of electrical properties of InAs oxide

We fabricated tunneling diode structures using AFM oxidation process as shown in Fig. 2 in order to study the electrical properties of the InAs oxide. After the removal of the AlGaSb/GaSb surface layers, two-terminal mesa structures were defined by electron-beam lithography using poly-methyl methacrylate (PMMA) and a successive wet chemical etching of the InAs channel and a part of the AlGaSb layer. The width of the mesa pattern is designed to be less than 1 μm in order to reduce the net area to be oxidized. The oxidation was then carried out immediately after the removal of the PMMA to minimize the formation of the native oxide on the InAs channel layer. The writing speed was 10 nm/s, and the tip voltage was 25 V. Other conditions such as the humidity were almost the same as those described in our previous report.[6] Finally, ohmic contacts were formed by an In/Au metalization and a lift-off.

The current-voltage (I-V) characteristics measured through the oxidized area showed a strong non-linear

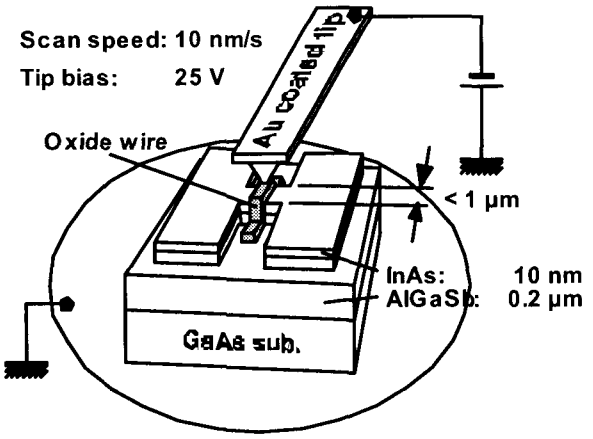

Fig. 2 Illustration of our AFM oxidation process of InAs. After the mesa structure formation, Oxidation is carried out by scanning the AFM tip across the narrow channel region.

behavior at room temperature while the two-terminal device without oxidation showed ohmic behavior. Therefore, the InAs regions left unoxidized act as a metallic contact, and the oxidized area, a tunneling barrier forming an MIM structure.

The I-V characteristics of the MIM structures were measured as a function of temperature between room temperature and 5 K. In Fig. 3, the I-V characteristics at temperatures of 50, 100, 150, 200, 250, and 300 K are plotted. As the temperature decreases, both the resistance and the breakdown voltage of the MIM structure increase from 300 K down to 200 K. For temperatures below 200 K, the breakdown voltage almost saturates because the tunneling current dominates

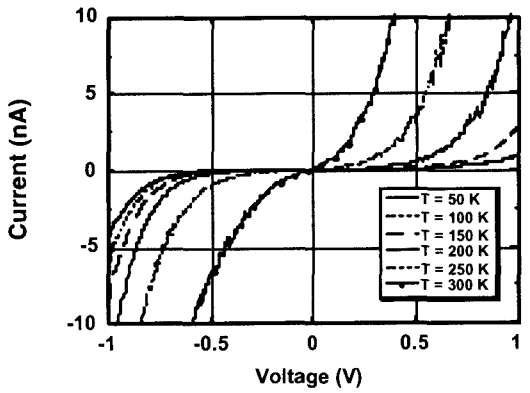

Fig. 3 Temperature dependence of the I-V characteristics measured for the MIM device shown in Fig. 2. The breakdown voltage increases as the measurement temperature decreases.

the I-V characteristics. The resistance at origin in Fig. 3 for T = 50 K is 15 G Ωthat is practically high enough as an insulator for most of device applications.

Thermionic-emission-current model was applied to

determine the barrier height of the InAs oxide. Figure 4 is the temperature dependence of the conductivity taken at bias voltages of 0.1, 0.2, 0.3, 0.4, and 0.5 V. The barrier height was obtained by extrapolating the activation energies obtained at each bias voltage to zero bias voltage. The barrier height measured from the Fermi energy is determined to be 0.35 eV. Since the Fermi energy is about 0.1 eV for an InAs with the electron concentration in the middle 10^{17} cm^{-3}, the net barrier height is about 0.45 eV. The obtained value is consistent to the breakdown characteristics shown in Fig. 3. The fact that the oxidized InAs shows an insulating behavior is particularly useful for nanostructure device fabrication using InAs-based heterostructures as described in the following section.

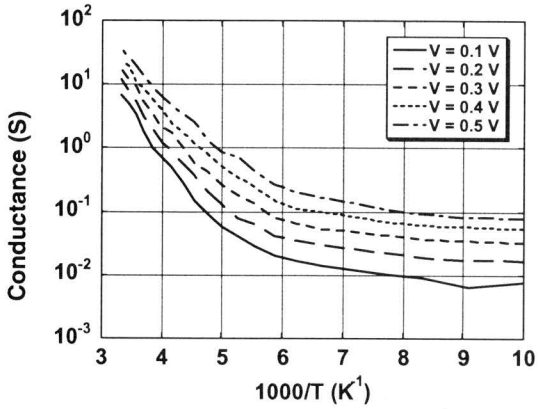

Fig. 4 Temperature dependence of the conductance for the MIM device shown in Fig. 2. Thermoionic-emission-model is applied to determine the activation energy for temperatures above 200 K.

4) SET fabrication using InAs oxidation process

In order to demonstrate the nanofabrication capability of this AFM oxidation, we fabricated single-electron transistor structures using an InAs/AlGaSb heterostructure. The thickness of the InAs channel layer is determined to be 10 nm to facilitate the oxidation. This reduces the tip voltage during oxidation and thus the tip wear. Therefore, the tip voltage for SET fabrication was fixed at 25 V for this experiment. An example of the SET structures is shown in Fig. 5. In the figure, brighter parts correspond to the oxidized areas thus insulating regions. An in-plane-gate structure is used for the SET fabrication. This is partly because the formation of good Schottky gate contacts on this material system has some difficulties. The SET channel is defined by a couple of parallel lines to form a narrow conducting channel between the source and drain. In the central part of the channel, two isolated islands are defined in series by three constrictions or tunneling barriers as shown in Fig. 5. By the introduction of direct oxidation of the InAs channel layer, a greatly simplified fabrication process is achieved. The effective island size is about 100 nm x 100 nm as is shown in the magnification of the island region.

The fabrication size obtained here enables the observation of quantum confinement effects in the fabricated devices since the effective mass of electrons in InAs is very small.

The SET characteristics were measured at 4.2K. A prominent oscillatory behavior due to Coulomb oscillations in the drain current as a function of gate voltage, Vg, was observed. The average period of the Vg was about 130 mV. In order to confirm the SET operation, a contour plot for the drain current with

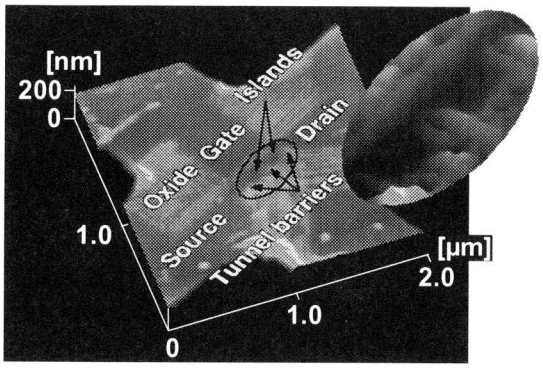

Fig. 5 AFM image of an SET fabricated by InAs oxidation process. Two islands defined by three constrictions are shown in the magnification.

respect to the gate and source-drain voltage was made and is shown in Fig. 6. As the gate voltage is decreased from –0.7 V, the current suppressed region shown by gray area once expands and then shrinks for Vg = -0.82 V. Therefore, a clear diamond structure is observed in this gate voltage range indicating the successful formation of the InAs SET and the feasibility

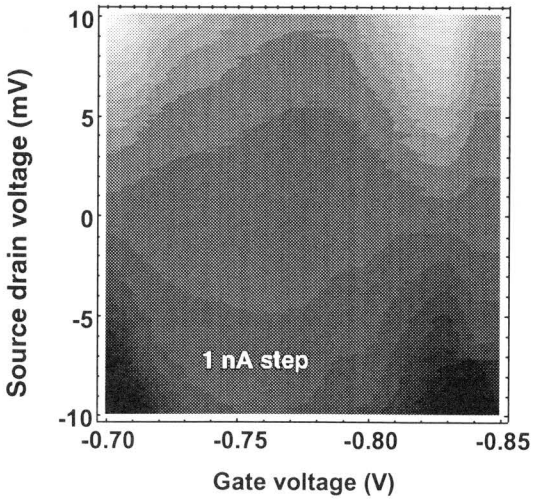

Fig. 6 Gray-scale plot for I_D with respect to V_G and V_{DS}. Adiamond structure is clealy observed indicating the successful formation of an InAs SET.

for nanostructure device fabrication of this AFM oxidation process. The Coulomb oscillations observed in this SET was not as regular as those observed in metalic systems. This is probably due to the interplay between charging and quantum confinement effects.

III. Conclusion

We described AFM oxidation process developed for the fabrication of InAs/Al(Ga)Sb heterostructures in the nanometer scale range. We studied the oxidation characteristics of InAs layers and found that oxidized InAs becomes an insulating material with the conduction band discontinuity of 0.45 eV with respect to InAs. By employing the InAs oxide for both gate insulators and tunneling barriers, an SET structure with in-plane-gate electrodes and two isolated islands was fabricated on an InAs/AlSb heterostructure. Successful SET operations verified by Coulomb oscillations and diamond structure demonstrate the simplicity and nanofabrication capability of this AFM oxidation. We also demonstrated that observable quantum confinement effects are attainable in InAs-based nanostructures using this AFM oxidation process.

Acknowledgments

The authors wish to thank A. Nakashima for device fabrication and characterization and M. Karasaki, and T. Kita for their MBE growth of the samples. This work was partly supported by a Grant-in-Aid for Scientific Research (C).

References

[1] J. A. Dagata, J. Schneir, H. H. Harary, C. J. Evans, M. T. Postek, and J. Bennett, "Modification of hydrogen-passivated silicon by a scanning tunneling microscope operating in air" Appl. Phys. Lett. **56**, 2001 (1990).

[2] E. S. Snow, P. M. Campbell, and B. V. Shanabrook, "Fabrication of GaAs nanostructures with a scanning tunneling microscope", Appl. Phys. Lett. **63**, 3488 (1993).

[3] M. Ishii and K. Matsumoto, "Control of current in 2DEG channel by oxide wire formed using AFM", Jpn. J. Appl. Phys. **34**, 1329 (1995).

[4] K. Matsumoto, M. Ishii, J. Shirakashi, K. Segawa, Y. Oka, B. J. Vartanian, and J. S. Harris, Tech. Dig. Int. Electron Device Meet., 363 (1995).

[5] S. Sasa, T. Sugihara, K. Tada, S. Izumiya, Y. Yamamoto, and M. Inoue, "High field transport properties of InAs/AlGaSb quantum wires", Physica B **227**, 363 (1996).

[6] S. Sasa, T. Ikeda, C. Dohno, and M. Inoue, "Atomic Force Microscope Nanofabrication of InAs/AlGaSb Heterostructures", Jpn. J. Appl. Phys. **36**, 4065 (1997).

[7] S. Sasa, A. Ohya, S. Yodogawa, and M. Inoue, "Nanoscale oxidation of InAs and its device applications", 12th Int. Conf. on Indium Phosphide and Related Materials Williamsburg (2000) p. 205.